

A. DRUZHININ, E. LAVITSKA, I. MARYAMOVA, M. OSZWALDOWSKI^{1,2}, T. BERUS¹,
H.W. KUNERT³

Department of Semiconductor Electronics, Lviv Polytechnic University, Ukraine

¹Institute of Physics, Poznan University of Technology, Poland

²International Laboratory of High Magnetic Fields and Low Temperatures, Wroclaw, Poland

³Department of Physics, University of Pretoria, South Africa

Studies of Piezoresistance and Piezomagneto- resistance in Si Whiskers at Cryogenic Temperatures

The temperature dependence of the electrical resistance of silicon whiskers was studied as their piezoresistance and piezomagneto-
resistance at 4.2 K. A special technique was developed to study the whiskers in compressive and tensile strain. It was observed that the thermal strain due to the mounting of the whiskers on different substrates at helium temperatures may be high enough to ‘throw’ a crystal from the metallic side of the metal-insulator transition to insulating one and vice versa. A negative magneto-
resistance in p-type silicon whiskers was found at 4.2 K, but in uniaxial compression a transition from negative magneto-
resistance to ‘anomalous’ positive magneto-
resistance was observed. The possibility to apply a ‘giant’ piezoresistance found in the vicinity of the metal-insulator transition in strain gauges and pressure sensors having a very high sensitivity to the measured value is discussed.

Keywords: silicon whisker, impurity conductance, metal-insulator transition, piezoresistance, magneto-
resistance, piezomagneto-
resistance

(Received October 26, 2001; Accepted January 4, 2002)

1. Introduction

Extensive studies devoted to semiconductor whiskers, particularly silicon whiskers, are due to their high structural perfection and special morphology (e.g.: MORALES, LIEBER 1998; ZHANG et al. 2001). Moreover, the structural perfection of whiskers results in their excellent mechanical properties. Consequently whiskers are successfully applied in various mechanical sensors (VORONIN et al. 1992; DRUZHININ et al. 1999; MARYAMOVA et al. 2000).

The special behavior of p-type silicon at cryogenic temperatures, where it exhibits hopping conductance and change of sign in its piezoresistance, is very interesting. The crystalline perfection of the whiskers makes it possible to investigate contribution in the electrical conductance of the disorder caused by randomly distributed doping impurities separately from that due to dislocations in bulk crystals. Moreover, we believe that our experimental results on piezoresistance in such a model material will be useful in the experimental verification of the theory of an acceptor state in silicon and its change with mechanical stress in the region of impurity conductance (CHROBOCZEK et al. 1984).

The main aim of the work is to study the possibility of practical application of silicon whiskers in sensors operating at cryogenic temperatures. Namely, it was of a special interest to reveal the region of dopant densities where the “giant” piezoresistance could be observed while the whiskers exhibit their electrical conductivity not far from that at the room temperature. Another problem was to study the behavior of Si whiskers in strong magnetic fields at 4.2 K. The main purpose of these studies was to reveal the stable crystals as related

to the magnetic field influence and search for the possibility to develop multifunctional sensors based on the combined piezoresistance-piezomagnetoresistance effect.

To meet this goal it was necessary to study the mechanisms of the electrical transport, piezoresistance and piezomagnetoresistance in the doped silicon whiskers at cryogenic temperatures. The moderately and heavily doped crystals have been chosen because they manifest the best combination of the stress/strain sensitivity (gauge factor GF) and a reasonable temperature stability. The latter parameter could be expressed in form of the temperature coefficient of resistance (TCR) and the temperature coefficient of the gauge factor (TCGF).

2. Experimental

The samples were obtained by chemical transport reactions in a closed system. The whiskers grew as elongated regular prisms, hexahedral in the cross-section, with diameters between a few microns and a few tens of microns. The longitudinal axis of the crystals corresponds to the [111] crystallographic direction. The whiskers were doped during growth with boron of concentrations between 8×10^{17} and $1 \times 10^{19} \text{ cm}^{-3}$. The presence of gold and platinum as growth initiating impurities provided some compensation of acceptor impurities. For experimental purpose whiskers with diameters between 20 and 60 μm about 5 mm long were selected. Two pairs of electric contacts (current and potential) to the crystals were fabricated by the laser welding of $\text{Ø}30 \text{ }\mu\text{m}$ Pt microwire.

Because of the small dimensions of the whiskers a special technique has been developed for the stress imposing during experimental measurements.

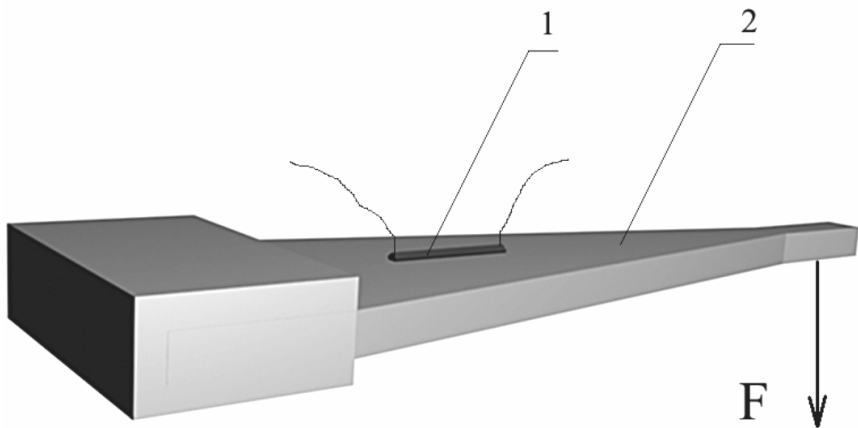


Fig. 1: Simplified view of the experimental set-up: (1) mounted crystal with corresponding lead wires; (2) cantilever.

Due to the small dimensions and typical shape of silicon whiskers it was not possible to apply mechanical loading directly to them. Therefore, the experiments on piezoresistance and piezomagnetoresistance were performed with samples mounted on specially fabricated substrates and elastic elements. In both cases the sample undergoes a thermal strain ϵ arising due to the difference in thermal expansion coefficients of the sample and the substrate.

Some measurements of piezoresistance and piezomagnetoresistance were made with the thermal strain only, while in other experiments external strain was applied. For this purpose a

special set-up fabricated on the basis of the helium cryostat was used. Silicon whiskers were mounted on cantilevers fabricated of Fe-Ni alloy (Fig. 1). The mounting was performed by viniflex adhesive VL-931 having a hardening temperature $T_0=460$ K.

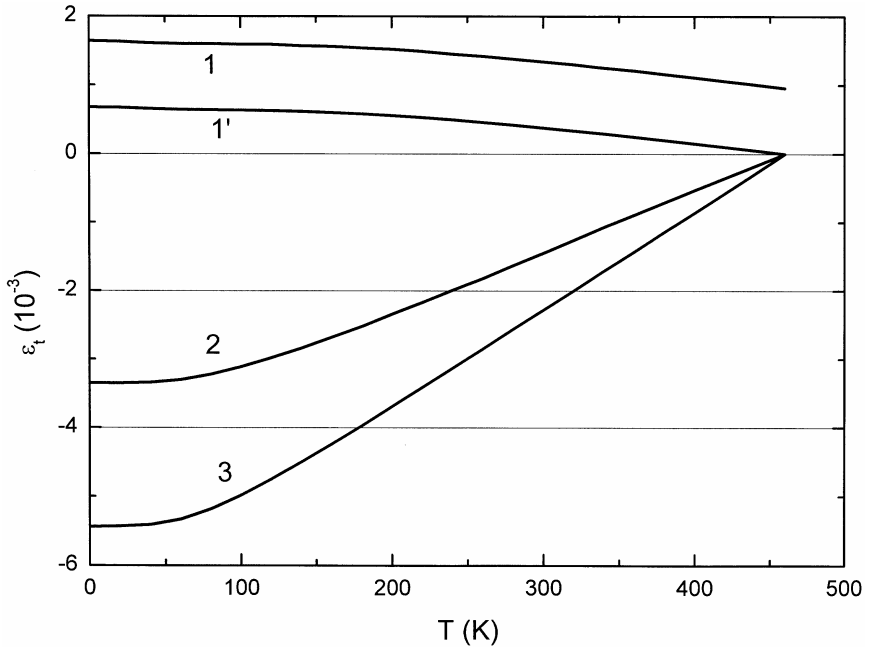


Fig. 2: Maximum ($g = 1$) thermal strain of a Si crystal mounted on substrates: (1,1') fused quartz, (2) steel and (3) copper. Temperatures of the adhesive hardening: (1) 770 K and (1',2,3) 460 K.

Table 1: Estimated maximum thermal strain of silicon whiskers mounted on different substrates.

Substrate	$T = 4.2$ K	$T = 20$ K	$T = 77$ K	$T = 300$ K
Cu	-5.44×10^{-3}	-5.43×10^{-3}	-5.18×10^{-3}	-2.28×10^{-3}
steel	-3.35×10^{-3}	-3.35×10^{-3}	-3.22×10^{-3}	-1.45×10^{-3}
fused quartz	6.77×10^{-4}	6.72×10^{-4}	6.40×10^{-4}	3.8×10^{-4}

During the experiment the cantilevers were elastically bent in four fixed steps. Since the cantilevers were significantly thicker as compared with the whisker transversal dimension, the whiskers were considered as purely tensioned or compressed, depending on the bending side of the cantilever. The linear external strain was estimated as (see e.g. ERLER, WALTER 1973):

$$e = \frac{3(l-x)h}{2l^3}d, \tag{1}$$

where l is the distance between the fixed edge of the cantilever and the point of the applied external force, x is the distance between the fixed edge of the cantilever and the central point

of the whisker, h is the thickness of the cantilever, and δ is the maximum displacement of the cantilever under the applied force (Fig. 2).

When mounting a whisker on the substrate with different thermal expansions coefficient using an adhesive with a hardening temperature T_0 one should expect the whisker at temperature T to be subjected to the thermal strain \mathbf{e}_p , which can be estimated in an isotropic approach as (LAVITSKA 1998):

$$\mathbf{e}_i(T) = \mathbf{g} \int_{T_0}^T [\mathbf{a}_s(T) - \mathbf{a}_c(T)] dt \quad (2)$$

where $\mathbf{a}_s(t)$ and $\mathbf{a}_c(t)$ are the thermal expansion coefficients of the substrate and the sample respectively. The dimensionless factor \mathbf{g} characterizes the strain transmission from the substrate to the sample. It may be determined experimentally (Appendix A) and estimated analytically (Appendix B). The value of \mathbf{g} depends on the experimental set-up and the sample geometry. An example of the $\mathbf{e}(T)$ estimation for silicon whiskers mounted on various substrates is shown in Fig. 2, while the corresponding numerical data are given in Table 1.

3. Results and discussion

At cryogenic temperatures the resistivity \mathbf{r} of doped semiconductors can be approximated as a sum of three resistivities \mathbf{r}_i with corresponding activation energies E_i (SHKLOVSKII, EFROS 1984):

$$\mathbf{r}^{-1} = \sum_{i=1}^3 \mathbf{r}_i^{-1} \exp(-E_i / kT), \quad (3)$$

where E_1 is the ground state ionization energy of the an impurity (acceptor, in our case) and E_2 and E_3 represent the ionization energies for the impurity conductance, i.e. activation energy E_3 for the hopping conductance and the activation energy E_2 for the hopping conductance due to the carriers in the band composed of the doubly occupied impurity states (A^+ in p-type semiconductors).

The samples studied here were related with three regions of the doping impurity boron concentration N_B close to the MIT:

- (i) insulating side of the MIT with $N_B < N_c$, where the critical concentration of the MIT $N_c \approx 5 \times 10^{18} \text{ cm}^{-3}$;
- (ii) metallic side of the MIT $N_B > N_c$;
- (iii) the vicinity of the MIT $N_B \gg N_c$.

Those three groups are clearly represented by the $\Delta \mathbf{r}(\mathbf{e}) / \mathbf{r}(0)$ curves vs uniaxial strain \mathbf{e} in Fig. 3.

When considering the temperature dependence of silicon samples mounted on substrates, one should take into attention two main effects which contribute to $\mathbf{r}(T)$: (i) temperature dependence of $\mathbf{r}(T)$ due to thermal activation process, carrier scattering, etc., and (ii) piezoresistance effect. The latter effect, in turn, is defined by the temperature variation of both piezoresistance coefficients and thermal strain of the sample.

In Fig. 3a sample 3 has metallic conductance and at cryogenic temperatures has positive longitudinal gauge factor in [111] direction, that is typical for heavily acceptor doped silicon: $G_{[111]} = (dR_{[111]} / R_0 \mathbf{e}) > 0$. Boron concentration in sample 1 corresponds to the insulating side

of the MIT with a negative gauge factor. Sample 2 having a small metallic behavior at small compressive strains becomes insulating at higher compressive loading. The sample shown in Fig. 3b behaves similarly, where the arrows indicate minima on the curves corresponding to the MIT. Transverse magnetic field shifts the minimum and acts in the same way as the uniaxial compression, shifting the sample behavior closer to the MIT.

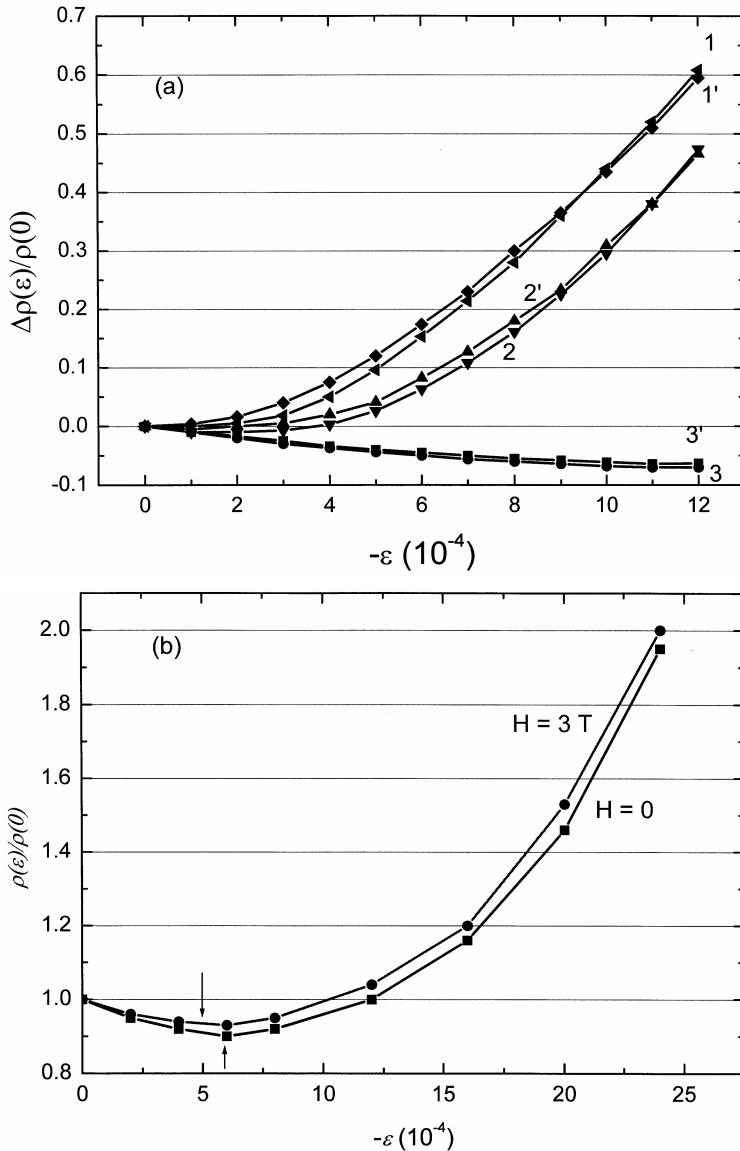
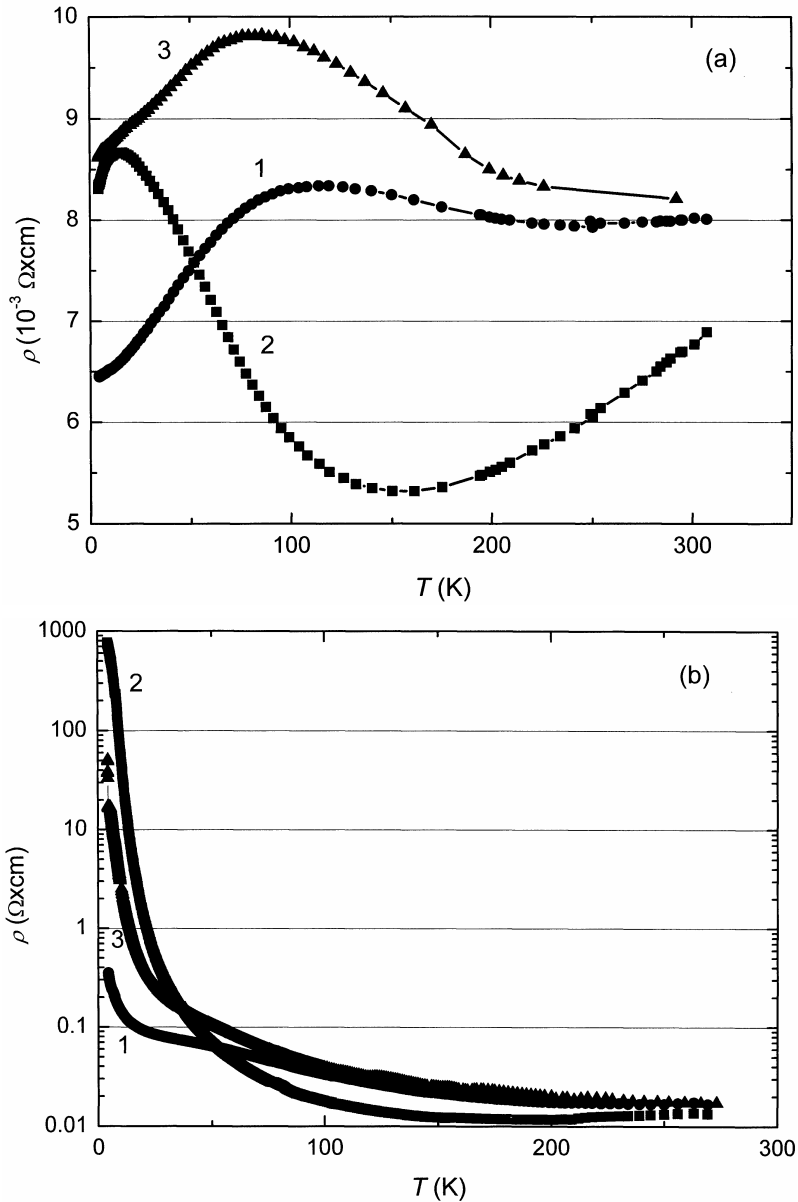


Fig. 3: Relative change of resistivities of Si whiskers with external uniaxial strain at 4.2 K: (1-3) without magnetic field and (1'-3') in magnetic field $H = 3$ T. Boron concentrations: (1,1') $N_B = 4 \times 10^{18} \text{ cm}^{-3}$; (2,2') $N_B = 6.6 \times 10^{18} \text{ cm}^{-3}$ and (3,3') $N_B = 9 \times 10^{18} \text{ cm}^{-3}$. In Fig. (b) the resistivity of the sample with boron concentration corresponding to the vicinity of the MIT ($N_B = 7 \times 10^{18} \text{ cm}^{-3}$) vs external uniaxial strain is shown without magnetic field and in magnetic field $H = 3$ T. Arrows show the minima in curves corresponding to the MIT.

Figures 4 a-c illustrate influence of the surface loading (Appendix A) due to the thermal stress on the temperature dependence of sample resistivities. Slightly metallic samples shown in Fig. 4a in the vicinity of the MIT demonstrate the non-monotonous temperature dependence of resistivity. Tensile strain from quartz substrate increases the resistivity in all the temperature range, while compressive strain from copper substrate decreases r at relatively high temperatures and provides its rise at lowest temperatures $T < 50$ K. Such a special behavior corresponds to the change in sign of the piezoresistance effect at the MIT region in compressive strain from positive to negative.



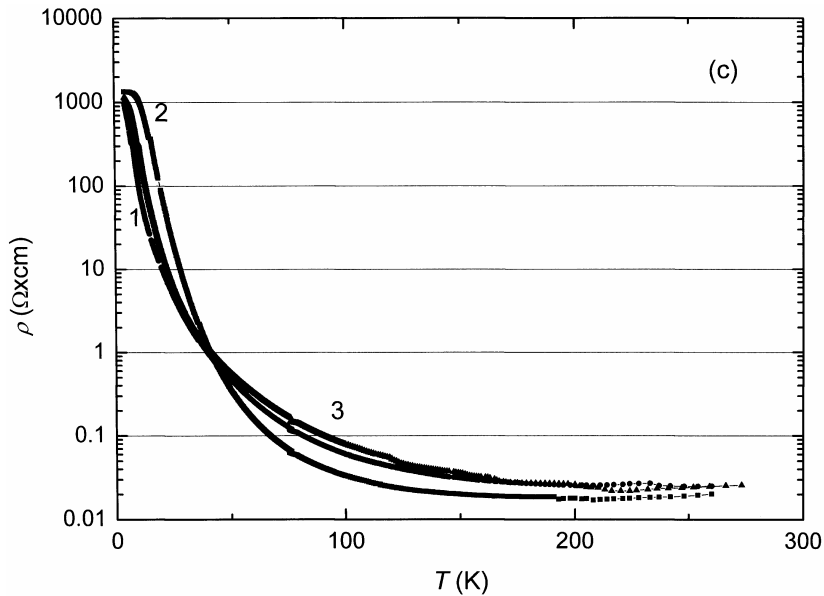


Fig. 4: Temperature dependence of resistivity of samples from different experimental sets with $N_B = 7 \times 10^{18} \text{ cm}^{-3}$ (a), $N_B = 3 \times 10^{18} \text{ cm}^{-3}$ (b) and $N_B = 8 \times 10^{17} \text{ cm}^{-3}$ (c): free (1), mounted on quartz (3) and copper (2) substrates.

However, the $\rho(T)$ dependences shown in Figs. 4b and 4c are monotonous in the entire temperature range and correspond to the insulating side of the MIT. The activation energies estimated from the temperature dependences of the samples with $N_B = 3 \times 10^{18} \text{ cm}^{-3}$ (Fig. 4b) at the different temperatures are given in Table 2.

Table 2: Activation energies E_2 for hopping conductance for the sample with $N_B = 3 \times 10^{18} \text{ cm}^{-3}$.

Sample montage	Temperature range (K) (type of an activation energy)	E_i (meV)
Free ($\epsilon=0$)	4.2-10 (E_3)	0.324
On Cu ($\epsilon=-5.44 \times 10^{-3}$)	4.2-6 (E_3)	2.325
	10-23 (E_2)	33.86
On quartz ($\epsilon=6.7 \times 10^{-4}$)	4.2-5.5 (E_3)	0.496
	8-27 (E_2)	16.39

Identification of the activation energies E_i from $\rho(T)$ dependence was performed according to their values, impurity concentration, and temperature range in agreement with the data from (CHROBOCZEK et al. 1984). A distinct dependence of the activation energies E_2 and E_3 on the applied stress for the samples at the insulating side of the MIT is evident from Table 2. Activation energy E_3 having the value below 1 meV was found in all the samples. It increases with strain applied independently on sign of this strain. The activation energy E_2 was found only in the mounted (strained) samples and it rises with the absolute value of the strain applied $|\epsilon|$. These results on the activation energy are in agreement with the theoretical analysis of the ground acceptor state in boron-doped silicon and experimental

data on the bulk material (CHROBOCZEK et al. 1984). From the strong dependence of activation energy on strain one can expect a large piezoresistance in the range of E_2 -conductivity. This expectation is confirmed by Fig. 4b, where the initial resistivity at 4.2 K changes by two order of value under tensile strain and even four order of value under high compression from copper substrate.

The data on very large piezoresistance obtained for the samples mounted on substrates are confirmed by the experiments with a similar sample ($N_B \approx 2 \times 10^{18} \text{ cm}^{-3}$) fixed on a cantilever (Fig. 5). Longitudinal gauge factor for these samples is about 10,000, which is approximately two order higher than in piezoresistors based on the heavily-doped Si crystals traditionally used at cryogenic temperatures (MARYAMOVA et al. 2000).

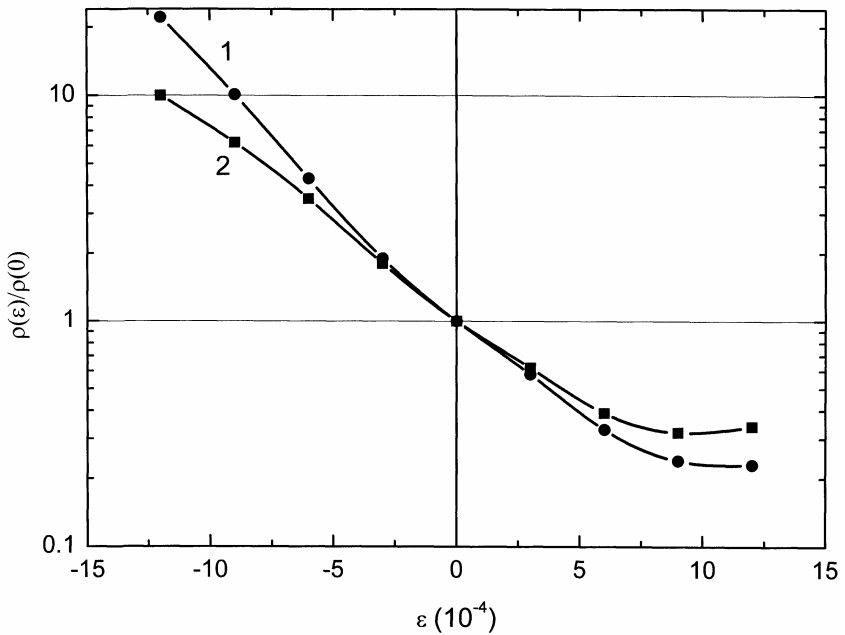


Fig. 5: Relative change of resistivity for Si whiskers vs external uniaxial strain at 4.2 for boron concentration $N_B = 2 \times 10^{18} \text{ cm}^{-3}$ (1) and $N_B = 2.3 \times 10^{18} \text{ cm}^{-3}$ (2). The case of the insulating side of the MIT.

The external strain of the samples in the vicinity to the MIT strongly influences their magnetoresistance (Figs. 6).

In metallic samples at certain levels of uniaxial compression oscillations in magnetoresistance are found (Fig. 6a) which vanish at higher stresses. This phenomenon may be explained in terms of crossing the Landau levels which appear in magnetic field by the Fermi level in heavily doped samples (Shubnikov-de Haas effect). Sufficiently high compression changes the distance between impurities and, thus, acts as a factor varying the effective doping of the crystal. The degree of degeneracy in the heavily doped samples decreases at high stress levels and, therefore, the oscillations disappear. A negative magnetoresistance has been found in boron-doped p-type silicon (Fig. 6b) which transforms to the so-called “anomalous” positive magnetoresistance at sufficiently high uniaxial compressions. Since this effect is observed only in the vicinity of the MIT (see also POLYANSKAYA et al. 1983), one attribute it to the variable-range hopping conductance on the

impurity states when resistivity depends on the temperature according to Mott's law:

$$r(T, H) = r_0(H) \exp [T_0(H) / T]^{1/4} \tag{4}$$

with the critical temperature of the MIT (SHKLOVSKII, EFROS 1984)

$$T_0(H) = \frac{b}{g(\mathbf{m}, H) x^3(H)}. \tag{5}$$

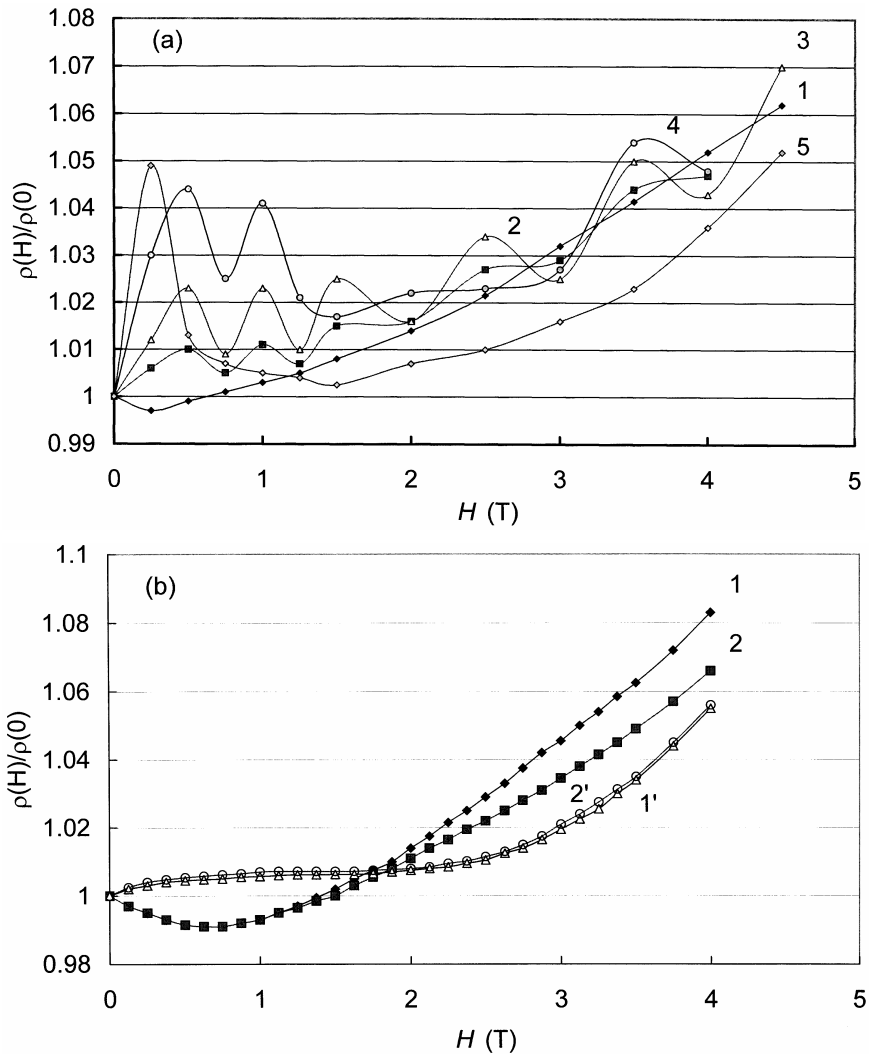


Fig. 6: Transversal magnetoresistance of boron-doped Si whiskers: (a) with boron concentration $N_B \approx 6.5 \times 10^{18} \text{ cm}^{-3}$ at different levels of external strain : $e=0$ (1), $e = -0.3 \times 10^{-3}$ (2), $e = -0.6 \times 10^{-3}$ (3), $e = -0.9 \times 10^{-3}$ (4), $e = -1.2 \times 10^{-3}$ (5); and (b) with $N_B \approx 5 \times 10^{18} \text{ cm}^{-3}$ at two levels of external strain: $e=0$ (1,2), $e = -1.2 \times 10^{-3}$ (1',2').

Here $g(\mathbf{m}H)$ is the density of states at the Fermi level, $\mathbf{x}(H)$ is an effective localization length at the impurity center, and \mathbf{b} is a numerical factor.

The only reason of the negative megnetoresistance is an increase of $g(\mathbf{m}H)$ that entails details of $T_0(H)$. However, the localization length $g(\mathbf{m}H)$ reduces with increasing magnetic field, causing the positive magnetoresistance. These two tendencies compete and at high magnetic fields positive magnetoresistance dominates (Fig. 8).

4. Concluding Remarks

The moderately doped silicon whiskers with $r_{300K} = 0.02 \text{ } \Omega\cdot\text{cm}$ showed monotonous $R(T)$ dependencies with sufficiently high temperature coefficient of resistivity. Variation in the resistance $(DR-R_0)/R_0$ in the temperature range between 4.2 and 300 K is about 10^5 , which makes these whiskers a suitable material for miniature low-inertial thermoresistors.

Ultra-high piezoresistance found in the whiskers (Figs. 4b, 5) at 4.2 K enables their use as sensitive elements of piezoresistive sensors (strain gauges, pressure sensors, and level sensors) operating at cryogenic temperatures (MARYAMOVA et al., 2000). The only limitation of these piezoresistive sensors is the temperature instability of their parameters. That is why it is recommended to apply such sensors at fixed temperatures, e.g. in cryogenic liquids, namely: liquid helium, liquid hydrogen etc. In particular, the developed pressure sensors were successfully tested during the pressure measurements in the cooling system of the super-conductive magnet. Another type of the developed piezoresistive pressure sensors based on heavily-doped whiskers with metallic-type conductance ($r \approx 0.005 \text{ } \Omega\cdot\text{cm}$) demonstrate a good stability of their parameters at cryogenic temperatures including conditions of high magnetic fields applied.

Appendix 1. Analysis of the surface strain/stress conditions

In the local coordinate system $\langle 111 \rangle$ the tensor of the surface thermal stress may be written in the following form:

$$(\mathbf{s}_{ij})'_{SURF} = \begin{pmatrix} \mathbf{s}_x & 0 & 0 \\ 0 & 0 & 0 \\ 0 & 0 & \mathbf{s}_z \end{pmatrix}, \quad (\text{A1})$$

where we direct Z axis along the longitudinal axis of a whisker, corresponding to the [111] crystallographic direction, while X axis lies in the same surface of the substrate and Y axis is normal to the surface of the substrate (Fig. A1).

Applying the known method (KUNERT, LAVITSKA 2001) to transform the components of a fourth rank tensor of elastic compliances, we obtaine for fcc {111} overlayer:

$$(S'_{ij}) = \begin{pmatrix} S'_{11} & S'_{12} & S'_{13} & S'_{14} & 0 & 0 \\ S'_{12} & S'_{11} & S'_{13} & -S'_{14} & 0 & 0 \\ S'_{13} & S'_{13} & S'_{33} & 0 & 0 & 0 \\ S'_{14} & -S'_{14} & 0 & S'_{44} & 0 & 0 \\ 0 & 0 & 0 & 0 & S'_{44} & S'_{14} \\ 0 & 0 & 0 & 0 & S'_{14} & S'_{66} \end{pmatrix} \quad (\text{A2})$$

with

$$\begin{aligned}
 S'_{11} &= \frac{1}{2}(S_{11} + S_{12} + 2S_{44}); & S'_{12} &= \frac{1}{6}(S_{11} + 5S_{12} - 2S_{44}); & S'_{13} &= \frac{1}{3}(S_{11} + 2S_{12} - 2S_{44}); \\
 S'_{14} &= \frac{\sqrt{2}}{12}(-S_{11} + S_{12} + 2S_{44}); & S'_{33} &= \frac{1}{3}(S_{11} + 2S_{12} + 4S_{44}); & S'_{44} &= \frac{1}{12}(S_{11} - S_{12} + 4S_{44}); \\
 S'_{66} &= \frac{1}{24}(S_{11} - S_{12} + 4S_{44}).
 \end{aligned}
 \tag{A3}$$

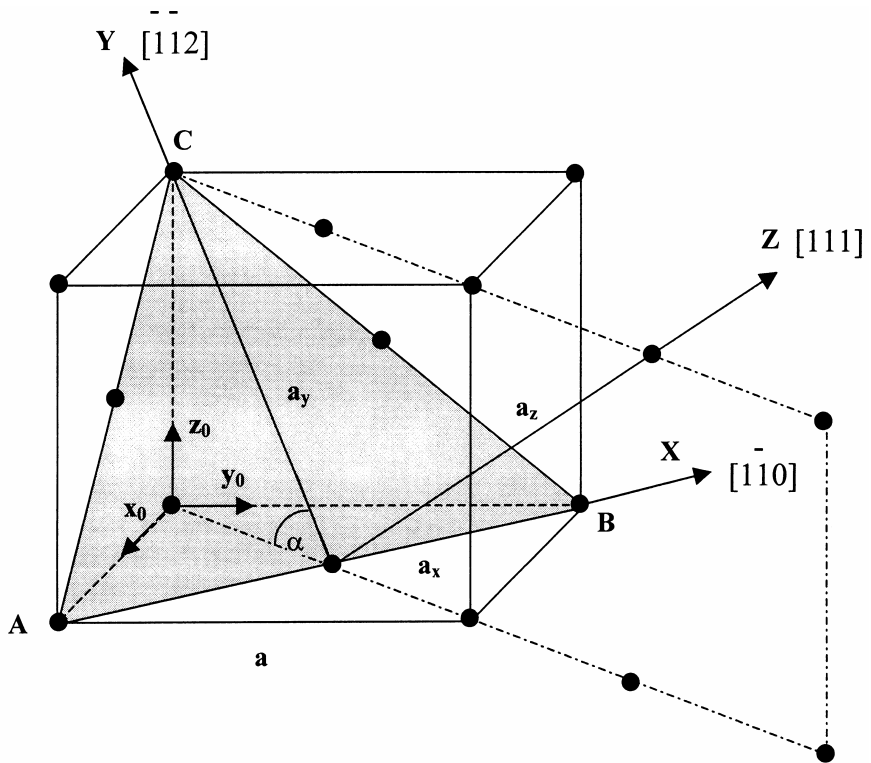


Fig. A1: Cubic cell of silicon with local coordinate axes.

From the stress tensor (A1) and the elastic compliances (A4) one can obtain the strain tensor corresponding to condition of the surface thermal stress:

$$\left(\mathbf{e}_{ij} \right)'_{SURF} = \left(S_{ijkl} \right)' \left(\mathbf{s}_{kl} \right)'_{SURF} = \begin{pmatrix} (S'_{11}\mathbf{s}_x + S'_{13}\mathbf{s}_z) & 0 & 0 \\ 0 & (S'_{12}\mathbf{s}_x + S'_{13}\mathbf{s}_z) & \frac{1}{2}S'_{14}\mathbf{s}_x \\ 0 & \frac{1}{2}S'_{14}\mathbf{s}_x & (S'_{13}\mathbf{s}_x + S'_{33}\mathbf{s}_z) \end{pmatrix}. \tag{A4}$$

For a crystal having a cubic symmetry and mounted on an anisotropic substrate one can expect the \mathbf{e}_{11} and \mathbf{e}_{33} components of the strain tensor (A4) to be equal. This gives a relation between \mathbf{s}_x and \mathbf{s}_z components:

$$\mathbf{s}_x = \frac{S'_{33} - S'_{13}}{S'_{11} - S'_{13}} \mathbf{s}_z, \quad (\text{A5})$$

or in terms of the known compliances S_{ij}

$$\mathbf{s}_x = \frac{12S_{44}}{S_{11} - S_{12} + 10S_{44}} \mathbf{s}_z = \mathbf{ks}_z = \mathbf{ks}. \quad (\text{A6})$$

Formulae (A1-A6) enable to estimate the piezoresistance effect due to the thermal strain in a mounted crystal. In particular, in such conditions of surface loading of the crystal the change in its resistance may be expressed in terms of the piezoresistance tensor (\mathbf{p}_{ijk}), which, after transformation to the local $\langle 111 \rangle$ axes, may be written in the form:

$$(\mathbf{p}_{ij})' = \begin{pmatrix} \mathbf{p}'_{11} & \mathbf{p}'_{12} & \mathbf{p}'_{13} & \mathbf{p}'_{14} & 0 & 0 \\ \mathbf{p}'_{12} & \mathbf{p}'_{11} & \mathbf{p}'_{33} & -\mathbf{p}'_{14} & 0 & 0 \\ \mathbf{p}'_{13} & \mathbf{p}'_{33} & \mathbf{p}'_{33} & 0 & 0 & 0 \\ \mathbf{p}'_{14} & -\mathbf{p}'_{14} & 0 & \mathbf{p}'_{44} & 0 & 0 \\ 0 & 0 & 0 & 0 & \mathbf{p}'_{44} & \mathbf{p}'_{14} \\ 0 & 0 & 0 & 0 & \mathbf{p}'_{14} & \mathbf{p}'_{66} \end{pmatrix} \quad (\text{A7})$$

with

$$\begin{aligned} \mathbf{p}'_{11} &= \frac{1}{2}(\mathbf{p}_{11} + \mathbf{p}_{12} + 2\mathbf{p}_{44}); & \mathbf{p}'_{12} &= \frac{1}{6}(\mathbf{p}_{11} + 5\mathbf{p}_{12} - 2\mathbf{p}_{44}); & \mathbf{p}'_{13} &= \frac{1}{3}(\mathbf{p}_{11} + 2\mathbf{p}_{12} - 2\mathbf{p}_{44}); \\ \mathbf{p}'_{14} &= \frac{\sqrt{2}}{6}(-\mathbf{p}_{11} + \mathbf{p}_{12} + 2\mathbf{p}_{44}); & \mathbf{p}'_{33} &= \frac{1}{3}(\mathbf{p}_{11} + 2\mathbf{p}_{12} + 4\mathbf{p}_{44}); & \mathbf{p}'_{44} &= \frac{1}{3}(\mathbf{p}_{11} - \mathbf{p}_{12} + 4\mathbf{p}_{44}); \\ \mathbf{p}'_{66} &= \frac{1}{6}(\mathbf{p}_{11} - \mathbf{p}_{12} + 4\mathbf{p}_{44}). \end{aligned} \quad (\text{A8})$$

Thus, the relative change in the resistances $(dR_i)' = (\Delta R_i / R_0)'$ in a matrix form may be expressed as:

$$(dR_3)'_{SURF} = \frac{1}{3} \left[\frac{S_{11} - S_{12} + 22S_{44}}{S_{11} - S_{12} + 10S_{44}} (\mathbf{p}_{11} + 2\mathbf{p}_{12}) + 4 \frac{S_{11} - S_{12} + 4S_{44}}{S_{11} - S_{12} + 10S_{44}} \mathbf{p}_{44} \right] \mathbf{s} \quad (\text{A9})$$

with $\mathbf{s} = \mathbf{s}_z$.

Derivations for conditions of the pure uniaxial stress

$$(\mathbf{s}_{ij})'_{UNI} = \begin{pmatrix} 0 & 0 & 0 \\ 0 & 0 & 0 \\ 0 & 0 & \mathbf{s} \end{pmatrix} \quad (\text{A10})$$

give us the relation

$$(\mathbf{d}R_3)'_{UNI} = \mathbf{p}'_{33} \mathbf{s} = \frac{1}{3} [(\mathbf{p}_{11} + 2\mathbf{p}_{12}) + 4\mathbf{p}_{44}] \mathbf{s} . \quad (\text{A11})$$

Substitution of the numerical values of the elastic compliances for silicon (i.e. $S_{11} = 0.768 \times 10^{-11} \text{ Pa}^{-1}$; $S_{12} = -0.214 \times 10^{-11} \text{ Pa}^{-1}$; $S_{44} = 1.26 \times 10^{-11} \text{ Pa}^{-1}$) in Eq. (A9) yields the following expression for the change of resistance in the [111] direction corresponding to the Z axis in the local coordinate system:

$$(\mathbf{d}R_3)'_{SURF} = \frac{1}{3} [3.84(\mathbf{p}_{11} + 2\mathbf{p}_{12}) + 3.22\mathbf{p}_{44}] \mathbf{s} . \quad (\text{A12})$$

Comparison of Eqs. (A11) and (A12) reveals that replacement of uniaxial stress by surface stress leads to a reduction in the shift component of piezoresistance related with \mathbf{p}_{44} by a factor of about 0.8 and to a significant (almost 4 times) increase in the hydrostatic component (related with $(\mathbf{p}_{11} + \mathbf{p}_{12})$).

It is known (SMITH 1954) that in p-type silicon in a wide range of temperatures and dopant concentrations, $\mathbf{p}_{44} \gg (\mathbf{p}_{11} + \mathbf{p}_{12})$. Consequently, changes in the resistivity given by Eqs. (A11) and (A12) are mainly defined by the second components related with the shear component of the stress. This means that contribution from the surface stress [Eq. (A1)] in the change in resistivity along the [111] axis is smaller than that from the uniaxial stress [Eq. (A10)]:

$$(\mathbf{d}R_3)'_{SURF} / (\mathbf{d}R_3)'_{UNI} \approx 0.8. \quad (\text{A13})$$

Comparison of $(\mathbf{d}R_3)'$ found from our experiments (Appendix 2) with the expected from uniaxial stress [Eq. (A10)] gives $(\mathbf{d}R_3)'_{\text{exp}} / (\mathbf{d}R_3)'_{\text{theoruni}} \approx 0.7$, that is in a reasonable accordance with Eq. (A13).

Appendix B. Method of experimental estimation of the thermal strain

Fig. B1a illustrates the principle of the experimental estimation of the thermal strain of a mounted crystal. Curve R_0 corresponds to the temperature dependence of the resistance of a free (unmounted) crystal. Curve $R_t(0)$ represents the temperature dependence of the resistance of the same crystal after mounting it on the cantilever at zero external strain. Other eight curves correspond to the $R(T, \epsilon)$ dependences at various levels of the external strain, both tensile (R_1, R_2, R_3, R_4) and compressive ($R_{-1}, R_{-2}, R_{-3}, R_{-4}$). The points where these $R(T, \epsilon)$ curves cross the R_0 curve correspond to the compensation of the thermal strain by the external one (i.e. $\epsilon_t + \epsilon_{\text{ext}} = 0$) and, therefore, one can determine exactly the temperatures where this compensation is achieved. Fig. B1b shows the dependence of thermal strain ϵ_t on temperature found from these experimental data.

The above method enables us to compare the analytical results on the estimation of thermal strain with experimental values of the strain. It was checked using the strain gauges with known gauge factor and proves its validity. The comparison of the experimentally determined ϵ_t at certain temperatures with that evaluated from Eq. (2) gave the dimensionless factor $g=0.7$. We used this value in the processing of our experimental data.

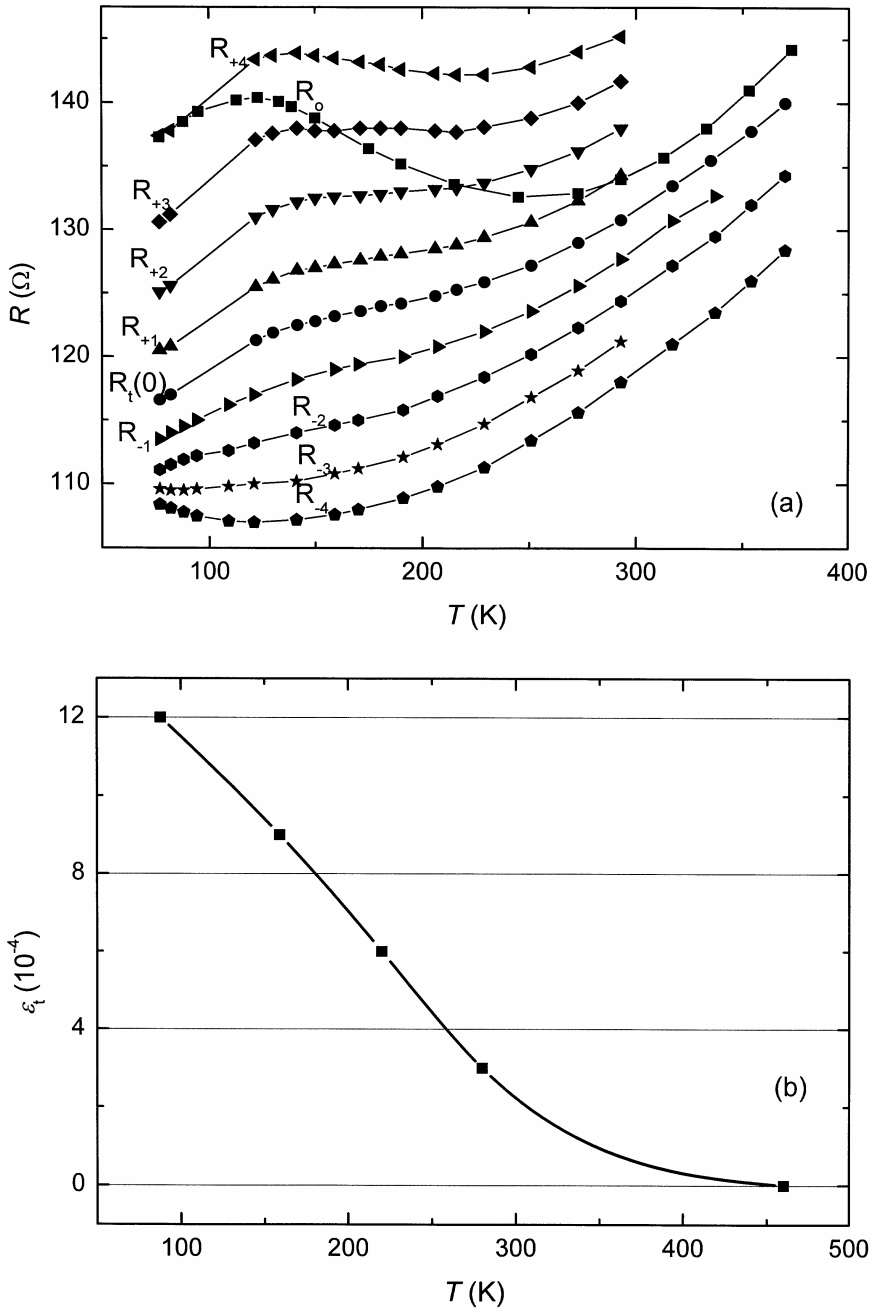


Fig. B1: (a) Temperature dependence of resistance of silicon whiskers: R_0 represents the experimental curve for the free (unmounted) crystal, while $R_t(0)$ the same sample mounted on a cantilever fabricated of Fe-Ni alloy. Numbers for other curves correspond to the following steps of the external strain: (R_{+1}) 1.2×10^{-3} , (R_{+2}) 0.9×10^{-3} , (R_{+3}) 0.6×10^{-3} , (R_{+4}) 0.3×10^{-3} , (R_{-1}) -0.3×10^{-3} , (R_{-2}) -0.6×10^{-3} , (R_{-3}) -0.9×10^{-3} , and (R_{-4}) -1.2×10^{-3} ; (b) Experimentally-determined thermal strain ϵ_t of Si crystal mounted on a substrate of Fe-Ni alloy.

References

- BIR, G.L., PIKUS, B.F.: Symmetry and Strain-Induced Effects in Semiconductors, Wiley, New York, 1974.
- CHROBOCZEK, J.A., POLLAK, F.H., STAUNTON, H.F.: Phil. Mag. 50 (1984) 113.
- DRUZHININ, A., LAVITSKA, E., MARYAMOVA, I.: Sensors and Actuators B58 (1999) 415.
- DRUZHININ, A., MARYAMOVA, I., HORTYNSKA, I., LAVITSKA, E., OSZWALDOWSKI, M.: Proc. SPIE 4413 (2001) 143.
- ERLER, W., WALTER, L.: Elektrisches Messen Nichtelektrischer Größen mit Halbleiterwiderständen, Veb Verlag Technik, Berlin, 1973.
- KUNERT, H.W., LAVITSKA, E.: Cryst. Res. Technol. 36 (2001) 1045.
- LAVITSKA, E.: Functional Materials. 5 (1998) 100.
- MARYAMOVA, I., DRUZHININ, A., LAVITSKA, E., HORTYNSKA, I., YATZUK, Y.: Sensors and Actuators A85 (2000) 153.
- MORALES, A.M., LIEBER, C.M.: Science 279 (1998) 208.
- POLYANSKAYA, T., SAIDASHEV, I., SHMARTSEV, Y.: Fizika i Technika Poluprovodnikov 17 (1983) 1081 (In Russian).
- SHKLOVSKII, B.I., FROS, A.L.: Electronic Properties of Doped Semiconductors, Springer-Verlag, Berlin-Heidelberg-New York, 1984.
- SMITH, C.S.: Phys. Rev. 94 (1954) 42.
- VORONIN, V., MARYAMOVA, I., ZAGANYACH, Y., KARETNIKOVA, E., KUTRAKOV, A.: Sensors and Actuators. A30 (1992) 27.
- ZHANG, Y., ZHANG, Q., WANG, N., YAN, Y., ZHOU, H., ZHU, J.: Journal of Crystal Growth 226 (2001) 185.

Contact information:

Prof. Dr. Anatoliy DRUZHININ, Dr. Elena LAVITSKA*, Dr. Inna MARYAMOVA
Department of Semiconductor Electronics, Lviv Polytechnic University
Kotlarevski street 1
Lviv 79013
Ukraine

Prof. Dr. Macej OSZWALDOWSKI, Ing. Tomasz BERUS
Institute of Physics, Poznan University of Technology
Ul. Nieszawska 13a, 61-022 POZNAN, Poland

Dr. Herbert-Willy KUNERT
Department of Physics, University of Pretoria
0002 Pretoria, South Africa

*corresponding author
e-mail: lavits@polynet.lviv.ua